Elements
An International Magazine of Mineralogy, Geochemistry, and Petrology

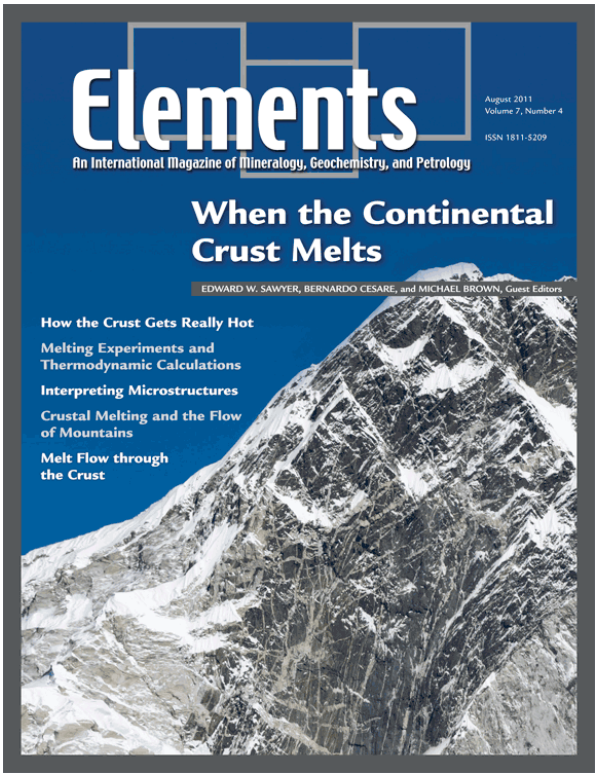

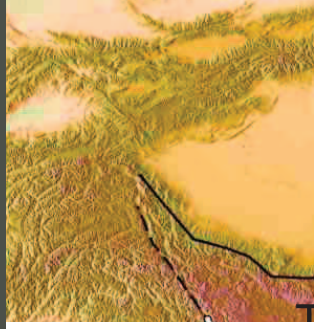

Crustal Melting and the Flow of Mountains

Rebecca A. Jamieson[1], Martyn J. Unsworth[2], Nigel B. W. Harris[3], Claudio L. Rosenberg[4], and Karel Schulmann[5]

1811-5209/11/0007-0253$2.50 DOI: 10.2113/gselements.7.4.253

As the continental crust thickens during mountain building, it can become hot enough to start melting, leading to a profound reduction in its strength. Melt-weakened crust can flow outward or upward in response to the pressure gradients associated with mountain building, and may be transported hundreds of kilometres laterally as mid-crustal channels. In the Himalayan–Tibetan system, melting began about 30 million years ago, and widespread granite intrusion began at 20–23 Ma. Geophysical data indicate that melt is present beneath the Tibetan plateau today, and deeply eroded mountain belts preserve evidence for melt-enhanced ductile flow in the past. Flow of partially molten crust may limit the thickness and elevation of mountain belts and has influenced the deep structure of continents.

KEYWORDS: crustal melting, mountain belts, ductile flow, melt-weakening, channel flow

INTRODUCTION

To most people, mountains appear strong and immutable, and the suggestion that mountain belts can flow may seem far-fetched. Nevertheless, there is overwhelming geological evidence for regional-scale ductile flow at depths of 30–50 km within the thickened regions of the Earth's crust, termed "orogens," that are characteristic of mountain belts. Geological evidence comes from metamorphic gneiss terranes in deeply eroded continental crust and recently exposed regions of young mountain belts. These rocks contain mineral assemblages and structures characteristic of flow on scales of tens to hundreds of kilometres at high temperature (≥700 °C) and pressure (≥800 MPa). In many cases, the rocks affected by ductile flow are migmatitic and have textures that indicate the presence of melt during deformation. In addition, laboratory experiments have demonstrated the profound effect of melting on rock strength, and geophysical measurements indicate that melt is present beneath a number of modern mountain belts, notably the Himalayan–Tibetan system. As a result, hypotheses have been proposed to link the presence of melt-weakened crust to ductile flow in both modern and ancient mountain belts.

1 Department of Earth Sciences, Dalhousie University Halifax, Nova Scotia B3H 4R2, Canada E-mail: beckyj@dal.ca

2 Department of Physics, University of Alberta Edmonton, Alberta T6G 2J1, Canada

3 Department of Earth and Environmental Sciences The Open University, Milton Keynes, MK7 6AA, UK

4 Department of Geological Sciences, Freie Universität Berlin Malteserstrasse 74-100, 12249 Berlin, Germany

5 EOST, Université Louis-Pasteur UMR 7517, 1 Rue Blessig, 67084 Strasbourg, France

In this article we review the experimental, geological, geophysical and geochemical evidence that melting and flow within mountain belts are widespread phenomena that have profoundly affected the evolution of the continents, and we discuss their effect on crustal thickening and mountain-building processes.

MAKING ROCKS FLOW – LABORATORY EXPERIMENTS

Since the late 1970s, laboratory experiments have demonstrated that rock strength, expressed as viscosity (Pa·s) or differential stress, $\Delta\sigma$ (MPa), decreases dramatically with increasing melt fraction. Early experiments on granitic samples with varying melt concentrations (e.g. Arzi 1978) pointed to a non-linear decrease in viscosity at melt volumes of 20–60% (FIG. 1A); the corresponding amount of melt was termed the *rheologically critical melt percentage* (RCMP). However, subsequent debate on the details of this phenomenon obscured the fact that the most significant viscosity reduction takes place at a much lower melt fraction (Rosenberg and Handy 2005), which becomes evident when strength is plotted on a linear scale. At melt volumes of 1–8%, the strength of rocks as measured in the laboratory decreases by ca 800–1000 MPa, or 90% of its initial value (FIG. 1B); in contrast, the absolute strength reduction associated with the RCMP is less than 10 MPa.

Application of these laboratory experiments to conditions found in the Earth must be undertaken with care, because deformation rates in the laboratory (ca 10^{-5}/s) are orders of magnitude faster than in nature (ca 10^{-13}/s). At different deformation rates, rocks deform by different mechanical processes, so that extrapolating laboratory results to nature may be invalid. For example, cataclastic (brittle) deformation is observed in almost all laboratory experiments performed at low melt fractions but is rarely observed in partially melted rocks in the field. This problem can be partly overcome by comparing theoretical predictions for deformation of melt-bearing rocks (e.g. Paterson 2001) with experiments on rocks that are less susceptible to cataclasis at low melt volumes (e.g. Rosenberg et al. 2007). This comparison confirms that the largest viscosity decrease takes place at melt volumes of 1–5%, with a second, less significant drop at 25–30%.

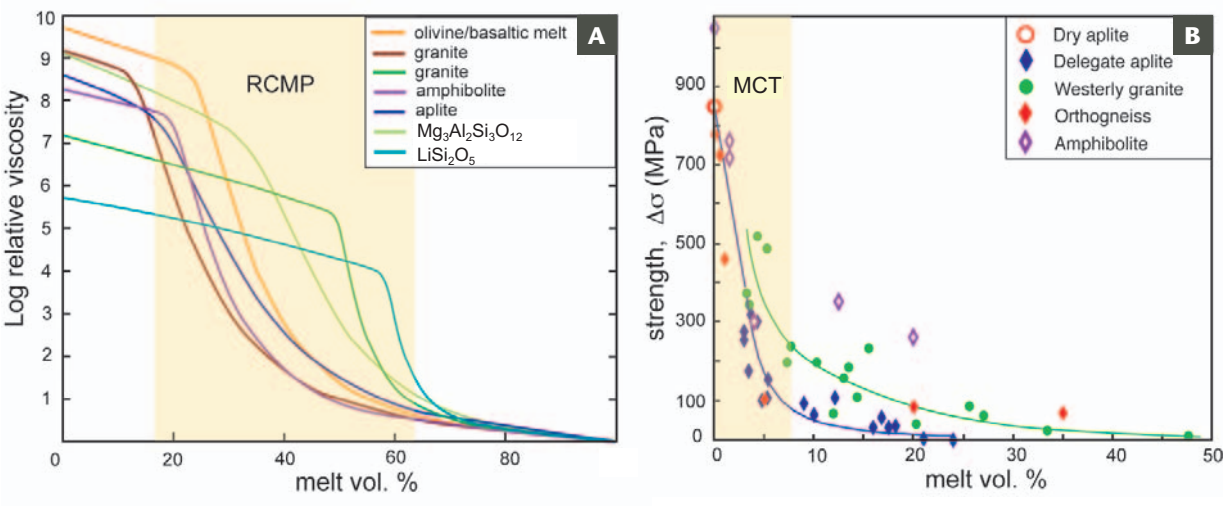

Figure 1 (**A**) Relative viscosity (aggregate viscosity/pure melt viscosity; note logarithmic scale) versus melt volume percent compiled from experimentally and empirically derived viscosities for a range of partially molten crust compositions (after Costa et al. 2009). The rheologically critical melt percentage (RCMP) occurs at 20–60% melt. (**B**) Strength (differential stress, Δσ; note linear scale) versus melt volume percent (after Rosenberg and Handy 2005). The melt connectivity threshold (MCT) occurs at ≤8% melt; the strength change at RCMP (<10 MPa) is too small to see in this plot.

Causes of the Two Strength Reductions

As a rock is heated, melt volume gradually increases, leading to two pronounced transitions in rheological behaviour. The exponential decrease in strength at less than 10% melt correlates with an increase in the connectivity of intergranular melt films (Rosenberg and Handy 2005; Fig. 1B). This is interpreted to cause the pattern of deformation to change from intracrystalline, that is, mainly within the interiors of strong grains, to intergranular, that is, localized in weak melt films along interconnected grain boundaries. This first rheological transition is therefore termed the *melt connectivity threshold* (MCT) (Fig. 1B; Rosenberg and Handy 2005). Between 10 and 20% melt, the rock consists of a continuous solid framework containing a network of interconnected melt channels with a structure resembling a sponge. The second significant strength reduction, at the RCMP, corresponds to the break-up of the solid-rock framework, which occurs at 20–60% melt, depending on strain rate and particle shapes (Costa et al. 2009). At higher melt volumes, the aggregate is no longer supported by a solid framework and behaves as a liquid with suspended unmelted grains.

Evidence for Melt-Weakening Processes in Rocks

Further insight into melt-weakening processes comes from microstructures in metamorphic rocks affected by melting during deformation (melt volume ca 10% at 750–800 °C, 700–1000 MPa). Studies of strongly deformed migmatitic and mylonitic rocks from the Bohemian Massif of central Europe (e.g. Schulmann et al. 2008b and references therein) suggest that both mechanical and chemical processes contribute to melt-weakening (Fig. 2). At high strain rates and low melt volumes, sliding along grain boundaries can produce cavities, leading to redistribution of melt and local volume increases (dilation).

In one example, melting reactions in quartzofeldspathic mylonites led to deformation by melt-enhanced sliding along grain boundaries and redistribution of melt into cavities (Fig. 2A), with granular flow at higher melt volumes. This caused unusual weakening of feldspar relative to quartz, as evident from extremely elongated feldspar aggregates (Fig. 2B). In a second example, melting reactions accompanying deformation of orthogneiss caused resorption of original crystals and precipitation of new ones, leading to disintegration of the original fabric and mixing of different minerals (Fig. 2C). Systematic variations in mineral composition and texture were interpreted to reflect continuous equilibration of deforming rock with infiltrating melt, possibly driven by dynamically created porosity linked to grain-boundary sliding, formation of cavities, and melt–rock reactions (Schulmann et al. 2008b). These observations are consistent with the suggestion that transient pulses of compaction and dilation contribute to melt migration and associated ductile flow in mid-crustal, partially molten rocks (e.g. Brown 2007).

Implications for Crustal Deformation

The decrease in viscosity with increasing melt fraction, characterized by the two rheological transitions described above, is predicted to have significant effects on small- and large-scale tectonic processes. Because even a small amount of melt produces a dramatic decrease in strength, incipient melting of the continental crust will inevitably lead to significant weakening and localization of deformation into melt-weakened migmatite zones. Large-scale detachments within migmatite layers probably develop during the first rheological transition (MCT) at low melt volumes. In active orogens, the large melt volumes (>20%) required to reach the RCMP threshold are unlikely to be achieved on a bulk scale in the melt-producing region because of efficient melt extraction and transfer during deformation (e.g. Brown 2007); however, this threshold may be exceeded where melts accumulate in the upper crust.

MAKING MOUNTAINS FLOW – NUMERICAL EXPERIMENTS

It is difficult to design realistic physical experiments that simulate crustal melting and deformation on the scale of mountain belts. Instead, sophisticated computer models are used to investigate many of the first-order processes involved, including crustal thickening, heating, melt-weakening, and the deformation associated with orogenic growth and ductile flow (e.g. Beaumont et al. 2001, 2006; Gerya et al. 2008; Rey et al. 2009). While different research groups use different computer algorithms and details of model design are widely debated, there is general agreement on the controlling processes and their effects on

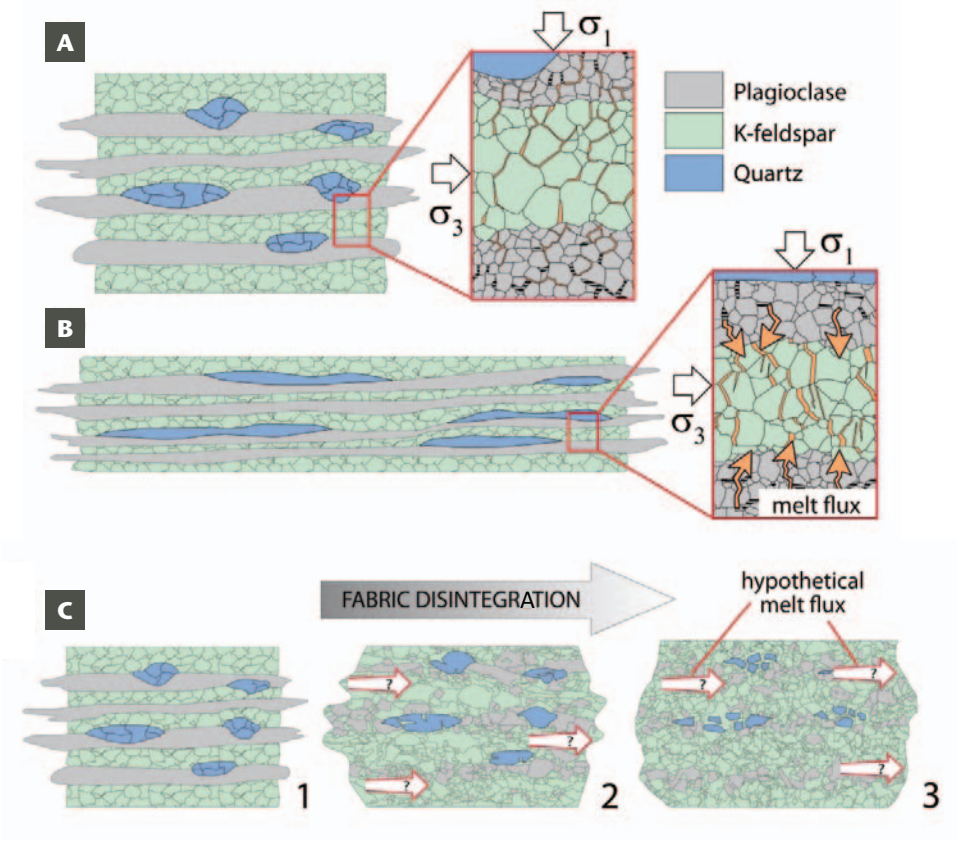

Figure 2 Schematic diagrams showing the different microphysical processes associated with melt-enhanced diffusion creep along grain boundaries and dislocation creep within grains (e.g. Schulmann et al. 2008b). σ_1, σ_3 = maximum and minimum principal stresses, respectively. (**A**) Melt produced by metamorphic reactions coats plagioclase grains and fills wedge-shaped pockets between K-feldspar grains. (**B**) Melt products are precipitated along grain boundaries and intragranular fractures in K-feldspar grains at a high angle to stretching lineations. (**C**) Progressive fabric disintegration and grain mixing result from melt infiltration and reactive porous flow.

large, hot orogenic systems. Here we describe a typical numerical experiment (reference model) and some simple variations, based on the work of Beaumont et al. (2001, 2006).

In the reference model, the crust is initially undeformed and consists of laterally uniform upper, middle, and lower crustal layers. The lower crust is stronger and has less radioactive heat production than the overlying crustal layers (Fig. 3). The underlying mantle lithosphere is strong and its motion may be predefined or calculated by the model. In the models described below, melt-weakening is treated as a linear reduction in viscosity from the nominal flow law value (typically 10^{20}–10^{21} Pa·s) to 10^{19} Pa·s over the temperature range 700–750 °C. This corresponds to the onset of muscovite dehydration melting and is also inferred to be equivalent to the melt connectivity threshold (MCT) described above. "Melt-prone" material in the models is any material to which this viscosity reduction is applied (upper and middle crust; lower crust is considered refractory) and that reaches the melt-weakening temperature range (≥700 °C). Crustal thickening is driven by convergence of one side towards the other, with the underlying mantle subducted beneath the orogen. The boundary between the two model continents, referred to as the "suture" (Fig. 3), would be marked in nature by remnants of the ocean basin that once separated the continents (e.g. ophiolites). As the crust thickens, it initially forms a pair of "back-to-back" thrust wedges facing in opposite directions on either side of the suture. The thickened crust is heated by radioactive decay, reaching T ≥ 700 °C in the middle and lower crust after about 20 million years (My) (Fig. 3A). With continued convergence, thickening, and heating, the crust eventually becomes too weak to sustain the topographic load and flows outward. This creates a flat orogenic plateau above the region of melt-weakened crust (Fig. 3B), flanked by wedges linking the plateau with stronger undeformed crust in the foreland.

The contrast in elevation between the plateau and the foreland (≥4 km) creates a pressure difference (gravitational potential energy gradient) capable of driving the flow of low-viscosity crust (≤10^{19} Pa·s) toward the foreland. The process is analogous to pressing on an egg sandwich: the soft filling is squeezed out and emerges at the edge of the sandwich and through any holes in the bread. In mountain belts, this "channel flow" takes the form of a tongue of melt-weakened crust (migmatite), bounded by lower thrust-sense and upper normal-sense ductile shear zones, and decoupled from and flowing between stronger lower and upper crust (Fig. 3B). The overlying crust may be transported with the flow, carrying its embedded structures, including the suture zone, with it; in this case, displacement on the upper normal-sense shear zone will be less than that on the lower thrust-sense shear zone. Where erosion rates are high at the orogenic flanks, the channel may be extruded at the surface (Fig. 3C). In this case, a traverse across the model from the foreland to the plateau would cross a fold and thrust belt, a zone of low- to medium-grade metamorphic rocks in which metamorphic grade increases upwards ("inverted" sequence), a ductile thrust-sense shear zone overlain by high-grade metamorphic rocks including deformed migmatites (extrusion zone; Fig. 3C), a zone of decreasing metamorphic grade associated with normal-sense ductile shear zones and faults, and finally low-grade to non-metamorphic rocks occupying the upper crust of the plateau (Figs. 3C, D). This pattern is reminiscent of the geology of the Himalayan Mountains (Figs. 4, 5; Jamieson et al. 2004).

The models are highly sensitive to variations in crustal strength. For example, upper crust that contains embedded weak layers (e.g. shale, salt) may develop instabilities that allow some channel material to flow vertically toward the plateau surface, creating structural domes cored by weak middle crust (Fig. 3D; Jamieson et al. 2006). Models with strength variations in the lower crust may not develop

continuous channel flow zones, but instead produce ductile nappes that are expelled towards the foreland when underthrust by stronger lower crust (Fig. 3E; Jamieson et al. 2007). In all models investigated to date, some form of melt-weakening is required to form broad plateaus associated with outward flow of weak crust from the core of the orogen towards its flanks. Models that lack melt-weakening form back-to-back thrust wedges (e.g. Willett et al. 1993) and do not develop plateaus or coeval thrust-sense and normal-sense shear zones.

The models described above are incomplete in that they do not incorporate the segregation, transport or emplacement of magma, nor do they include buoyancy effects. Melt-weakened regions in the model must therefore be considered zones of incipient partial melting (melt volume ≤ 10%) that flow in response to differential pressures within the deforming system. Where larger volumes of melt are present and can segregate efficiently (e.g. Brown 2007), the low density of the melt relative to its host rocks should promote buoyant vertical transport of magma, leading to emplacement of plutons and/or creation of melt-cored domes in the upper crust (e.g. Rey et al. 2009). Where melt-prone material becomes incorporated into the deep levels of an orogen, widespread melting could lead to buoyant vertical transport of lower crust (e.g. Lexa et al. 2011), in contrast to the dominantly lateral transport described above.

CRUSTAL MELTING IN THE EARTH'S LARGEST MOUNTAIN BELTS

As the one of the largest mountain belts that have ever existed on Earth, the modern Himalayan–Tibetan orogen (Fig. 4) is a natural laboratory for investigating the distribution of melt in an active orogen and for studying the melt products formed during its growth. Crustal thickening, driven by collision between India and Asia, began 50–55 million years ago. The Indian plate has been thrust under the Asian plate and its leading edge now lies under the Tibetan plateau, about 300 km north of the Indus–Tsangpo suture zone (ITS) that marks the surface position of the collision boundary (Figs. 4, 5; Nábělek et al. 2009). The present-day crustal thickness exceeds 80 km, and inferred temperatures in the middle to lower crust are well above 700 °C (Nelson et al. 1996; Klemperer 2006). Geological and geophysical evidence indicates that melting began at about 30 Ma and continues to this day.

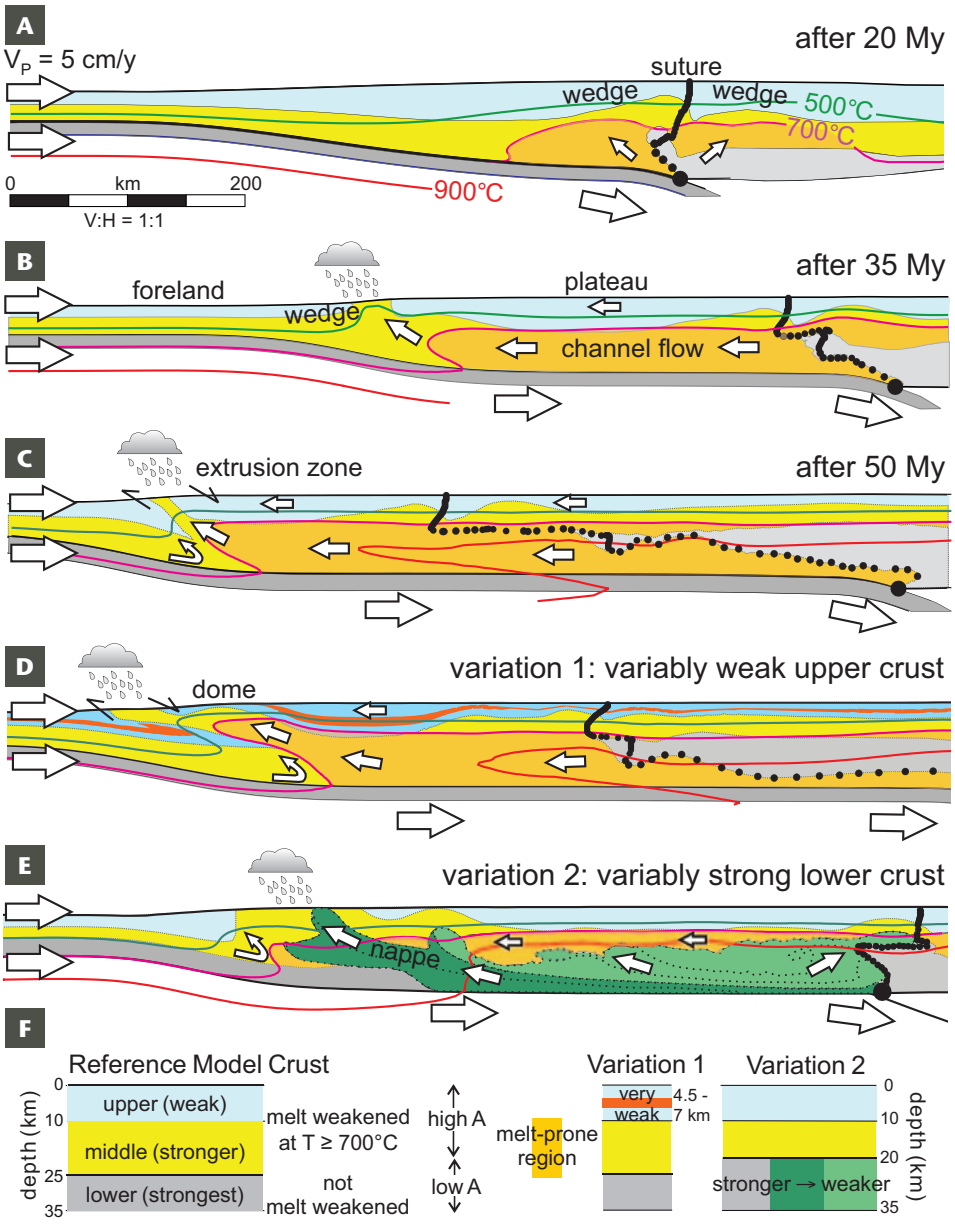

Figure 3 Numerical model predictions for crustal flow in reference model (A to C) and simple variations (D, E) for melt-weakened orogenic belts (after Beaumont et al. 2001, 2006; Jamieson et al. 2006, 2007); the time elapsed after initial collision is indicated in models A to C in millions of years (My). White arrows show the directions and relative magnitudes of flow. A melt-prone region (gold) lies between the 700 °C isotherm and the base of the middle crust. Black dots show the position of the suture. V_P = convergence velocity, A = radioactive heat production. (**A**) Crustal thickening forms back-to-back wedges and leads to heating in the orogenic core. (**B**) Melt-weakening leads to outward-directed channel flow, driven by the pressure gradient between the plateau and foreland (elevation difference ca 4 km). The upper crust and suture may be transported with the flow. (**C**) The channel is extruded between thrust- and normal-sense shear zones by focused erosion at the orogenic front. (**D**) Models with an embedded weak layer (orange) in the upper crust form wider orogens with broad extrusion zones and domes. (**E**) Models with variably strong lower crust (green) form ductile nappes, with limited channel flow beneath the plateau. (**F**) Properties of model materials

Geophysical Evidence for Melting beneath Tibet

Although surface mapping by geologists is the first step in understanding the structure of a mountain belt such as the Himalaya, determining the distribution of rocks and melt below the surface requires the use of geophysical imaging. The most widely used technique is seismic reflection, which uses sound (seismic) waves generated by explosions or earthquakes to determine the composition and depth of underground rock layers, much like medical ultrasound imaging is used to look inside the human body. The velocity of seismic waves varies according to rock composition, and the presence of fluids such as partial melt and brines lowers the velocity of both crustal and mantle rocks significantly. Since the 1980s, seismic surveys such as the INDEPTH profile (Figs. 4, 5A; Nelson et al. 1996) have revealed the deep crustal structure of the Himalayan–Tibetan orogen. The data clearly show the Indian plate dipping north beneath the Himalaya along the Main Himalayan Thrust (MHT; Fig. 5A). North of the ITS, a strong reflection at 15–20 km depth (B2 in Fig. 5A) provides evidence for a zone of crustal fluids that could be either partial melts or brines.

Magnetotelluric imaging uses natural radio waves to measure the electrical resistivity of the crust and mantle, which is very sensitive to the presence of fluids. Figure 5A shows results from a magnetotelluric survey made along the INDEPTH seismic profile in southern Tibet (Unsworth et al. 2005). Comparing the seismic and magnetotelluric data (Fig. 5A) shows that the underthrust Indian plate has the high electrical resistivity expected for old, cold lithosphere. In contrast, the crust beneath the Tibetan plateau has anomalously low resistivity, which is most reasonably explained by the presence of fluids. Moreover, the top of the low-resistivity layer coincides with seismic reflection B2, giving two lines of evidence for a zone of fluids at depth. Unsworth et al. (2005) concluded that 5–12% partial melt is probably required to explain the observed electrical resistivity of this layer. As discussed above, this volume of melt should cause a profound decrease in strength, sufficient to permit outward crustal flow under gravitational pressure (e.g. Clark and Royden 2000; Beaumont et al. 2001).

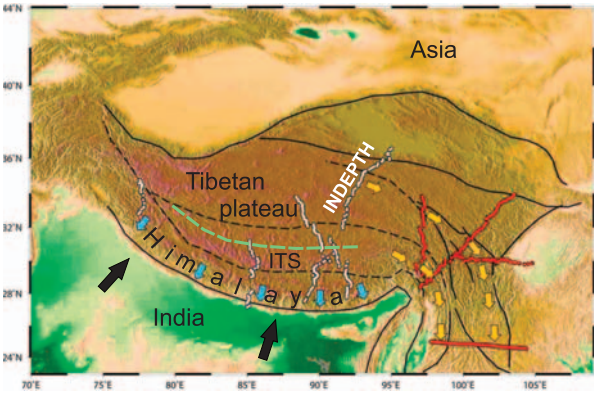

Figure 4 Digital elevation map of the Himalayan–Tibetan collision zone (after Royden et al. 2008; Nábělek et al. 2009; Bai et al. 2010), showing plate tectonic convergence (black arrows) and inferred outward flow of melt-weakened crust from beneath the Tibetan plateau toward the Himalaya (blue arrows) and southeast Asia (yellow arrows). ITS (black dashed lines) = Indus–Tsangpo suture zone. The red and white lines show the locations of seismic and magnetotelluric profiles described in the text, including the INDEPTH profile (Fig. 5A). The dashed green line shows the approximate limit of underthrust Indian crust (Nábělek et al. 2009).

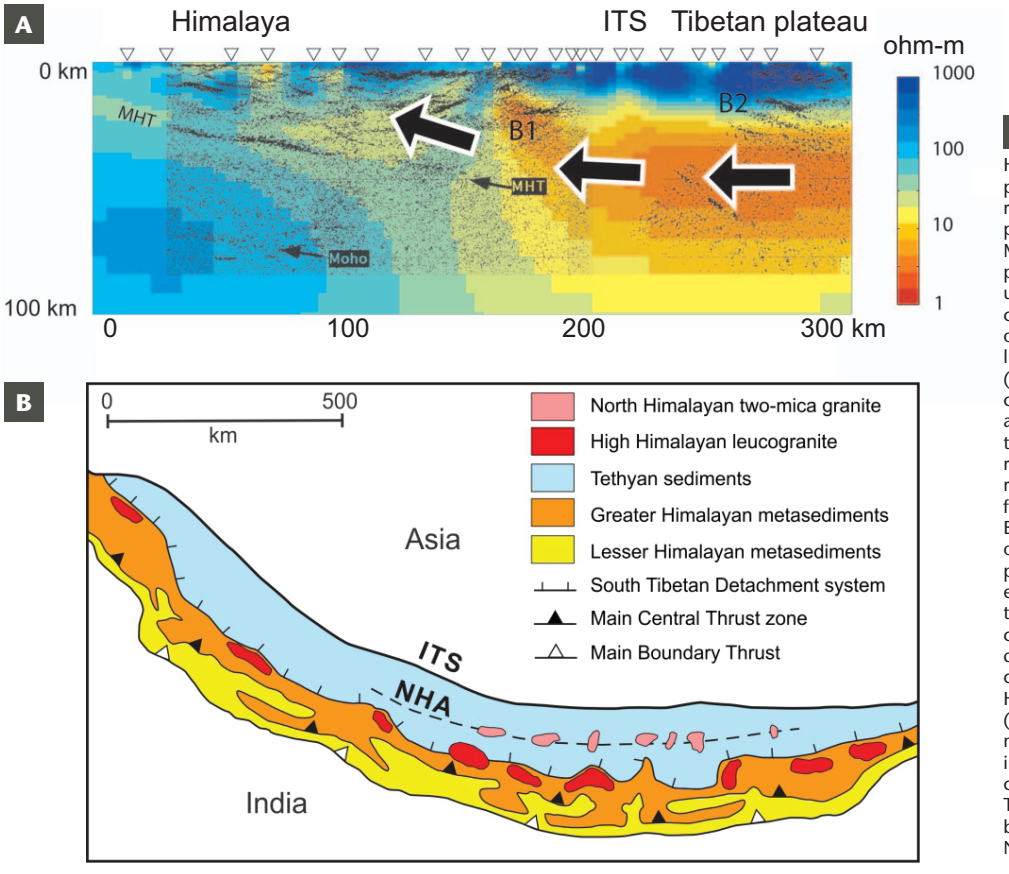

Figure 5 (**A**) Geophysical image of the crust below the Himalaya and southern Tibetan plateau. Black lines show seismic reflection data from the INDEPTH profile (Fig. 4; Nelson et al. 1996). MHT = Main Himalayan Thrust, interpreted as the upper surface of the underthrust Indian plate. Colour contours show electrical resistivity (in ohm-m) determined by magnetotelluric exploration on the same transect (Unsworth et al. 2005); triangles indicate data-recording locations. Blues and greens represent resistivity values typical of dry crust and upper mantle; red regions have anomalously low resistivity, indicating the presence of a fluid phase (e.g. partial melt); reflector B2 is interpreted to represent the top of a fluid-bearing region. Arrows show possible flow direction leading to exposure of mid-crustal melt zones in the High Himalaya. (**B**) Geology of the central Himalayan orogen showing distribution of plutons formed by crustal melting within the High Himalayan (red) and North Himalayan (pink) granite belts. Greater Himalayan metasediments (orange) have been interpreted to represent an extruded channel flow zone. ITS = Indus–Tsangpo suture (defines the plate boundary at the surface); NHA = North Himalayan antiform

Magnetotelluric and seismic surveys on the Tibetan plateau show that crustal layers with low resistivity and low seismic velocity are widespread below a depth of 15–20 km. Notably, the highest fluid contents, implying the highest degree of melting and thus locations where crustal flow may be possible, are found in two distinct regions. The first is in southern Tibet, extending along most of the east-west length of the Himalaya, where the flow is inferred to be in a southward direction and coupled to erosion in the Himalaya (Fig. 4; Beaumont et al. 2001). The second is in eastern Tibet, where horizontal movement of the crust is the dominant style of deformation now accommodating the India–Asia collision (e.g. Royden et al. 2008). Surface motion in this area is thought to be a response to outward flow of weak lower crust toward the southeast (Fig. 4; Clark and Royden 2000; Royden et al. 2008). This interpretation is supported by geophysical surveys that show elongated regions of low seismic velocity (Royden et al. 2008) and high fluid content (Bai et al. 2010) in the crust, which may be flow channels, shear zones, or both. Similar observations from other active mountain belts (Unsworth 2010) support the hypothesis that crustal melting during mountain building contributes to plateau formation and lateral flow of the crust.

Geological Record of Crustal Melting in the Himalaya

Granites and migmatites distributed over more than 1500 km along the length of the Himalayan orogen (Fig. 5b) reveal when and where the crust has melted since the India–Asia collision began. Most of this evidence comes from muscovite-bearing leucogranites that intruded Greater Himalayan gneisses and migmatites south of the High Himalaya (Fig. 5b; Harris 2007). The metamorphic rocks were transported from north to south as a ductile sheet bounded to the south (below) by the Main Central Thrust zone and to the north (above) by the normal-sense South Tibetan Detachment system (e.g. Beaumont et al. 2001; Harris 2007). Geochemical and petrological studies demonstrate that the High Himalayan leucogranites were derived from melting of their metasedimentary host rocks, driven by fluid-absent muscovite breakdown within the mid-crust (ca 20–30 km, 670–700 °C; Harris and Massey 1994). Based on the thermal properties of Himalayan rocks, numerical models and the distribution of leucogranites, it is thought that the high temperatures resulted from radioactive heat production within the thickened continental crust (Zhang et al. 2004). The ages of the leucogranites, determined from U–Pb dating of accessory minerals such as zircon and monazite, are key to understanding the relationship between crustal-scale deformation and crustal melting. Across much of the central Himalaya, leucogranites exposed today formed between 20 and 23 Ma, at about the same time as their host rocks were undergoing partial melting and about 30 My after the collision began. Evidence from mineral cooling ages indicates that they formed during a period of rapid exhumation, consistent with experimental evidence indicating that about 10% melting can be induced by decompression (Harris and Massey 1994). In the eastern Himalaya, granites as young as 11 Ma, interpreted to represent deeper levels of the crust, have been exposed by a combination of intense erosion and normal faulting at higher structural levels (e.g. Harris 2007).

In southern Tibet, a second belt of Tertiary granites was emplaced into the core of the North Himalayan antiform (Fig. 5b), where metamorphic gneiss domes are exposed within low-grade Tethyan sedimentary rocks. Doming of the mid-crust between the mountain front and the ITS is predicted by some models of mid-crustal channel flow beneath thin, weak upper crust (Fig. 3d; Beaumont et al. 2001; Jamieson et al. 2006). Recent studies have identified two distinct types of North Himalayan granites, distinguished by their petrology, field relations and emplacement ages. The younger group comprises porphyritic two-mica granite plutons emplaced between 15 Ma and 9 Ma, with isotopic and trace element compositions virtually indistinguishable from the High Himalayan leucogranites (Zhang et al. 2004). They are likely to have formed by a similar process, although their kyanite-bearing mineralogy and major element geochemistry suggest that melting occurred at somewhat deeper crustal levels (ca 30 km). The relatively young ages suggest rapid exhumation, perhaps related to the mid-Miocene development of the North Himalayan gneiss domes.

The older group of North Himalayan intrusions comprises equigranular, two-mica, garnet-bearing granites that form complex networks of sheets and dykes intruding the host rocks. Their emplacement between 28 and 23 Ma predated significant decompression of their host rocks, and their geochemistry suggests that a fluid phase was present during melting (King et al. 2011). Because fluid-saturated magma crystallizes when the pressure drops (e.g. Harris and Massey 1994), these melts would not have risen significantly from their source before they crystallized and would have formed sheet-like conformable bodies rather than cross-cutting diapiric plutons. Recognition of this older suite of intrusions, which are coeval with top-to-the-south shear fabrics but predate shear-sense reversal, places important constraints on the timing of southward flow of mid-crustal rocks beneath southern Tibet (King et al. 2011). Their ages approximately coincide with numerical model predictions that crustal melting and channel flow within the Himalayan orogen began at ca 30 Ma (Beaumont et al. 2001, Jamieson et al. 2004; Fig. 3a), a prediction made several years before crust-derived granites of this age were first documented.

Lifting the Lid – Evidence of Flow in Ancient Mountain Belts

In deeply eroded continental regions, the middle to lower crust of ancient orogenic belts is now exposed at the surface, allowing geologists to study features that are hidden from view beneath modern plateaus. In many cases there is overwhelming evidence that melt was present in the deforming crust, and its presence must therefore have affected both crustal strength and tectonic style. Good examples come from two ancient orogenic belts that once rivalled the Himalaya in scale: the Paleozoic Variscan orogen in Europe and the Proterozoic Grenvillian orogen in North America.

The European Variscan orogen formed at 430–300 Ma during progressive accretion of peri-Gondwanan blocks to the Laurussian continent (Schulmann et al. 2009). In what is now the Bohemian Massif, subduction of continental crust led to formation of felsic granulites and eclogites within a hot (850–1000 °C), deep (60–70 km) orogenic root zone. Subsequent shortening led to vertical material transfer of lower crustal diapirs to the mid-crust (Lexa et al. 2011), accompanied by decompression melting that transformed the exhuming lower crust into a partially molten mush containing refractory bodies of high-pressure rocks. Ascending migmatitic lower crust initially pooled at depths of 10–25 km beneath a rigid lid and then flowed laterally, leading to detachment and partial fragmentation of the lid. Subsequent indentation of the orogenic root by stronger lower crust activated a thick, hot, ductile sheet that was transported 200 km as a heterogeneous channel flow (Fig. 6; Schulmann et al. 2008a; Lexa et al. 2011). The hot,

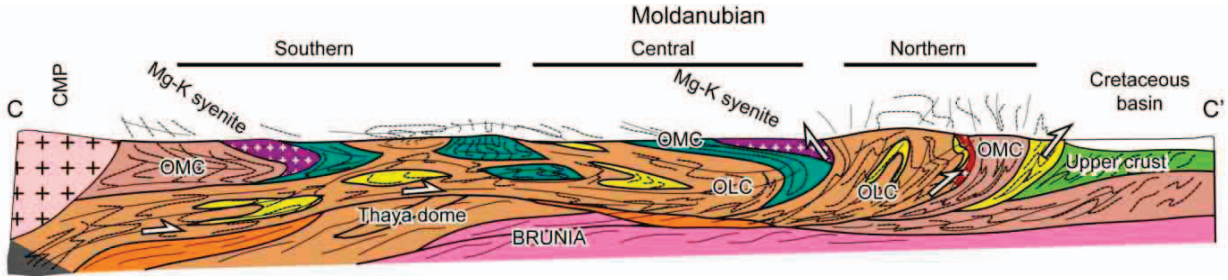

Figure 6 Inferred heterogeneous channel flow within the Moldanubian region, Bohemian Massif, in the Variscan orogen of central Europe (after Schulmann et al. 2008a, Lexa et al. 2011). Melt-weakened lower crust (beige), carrying blocks of high-pressure and high-temperature rocks (yellow) and orogenic middle crust (green and orange), flowed over strong continental crust (Brunia, pink) during late Paleozoic collision. CMP = Central Moldanubian Pluton; OMC = orogenic middle crust; OLC = orogenic lower crust

migmatitic flow zone transported blocks of deep orogenic lower crust (granulites and eclogites) and heated adjacent mid-crustal metasediments. The short-lived (5–10 My) channel flow episode was accompanied by deep erosion of the orogenic lid.

The Grenvillian orogen of eastern North America formed between 1200 and 1000 Ma during convergence between the Laurentian and Amazonian continents (e.g. Jamieson et al. 2007 and references therein). Gneisses and migmatites that formed at 25–35 km depth and 700–900 °C are widely distributed within this deeply eroded mountain belt. In central Ontario, migmatite containing up to 30% leucosome formed during convergence and persisted in the mid-crust for 20–40 My (Slagstad et al. 2005). Field relations indicate that this melt-weakened crust formed thin lobate sheets that flowed laterally for tens of kilometres. However, the overall style of melt-enhanced ductile flow more closely resembles stacking of ductile nappes (Fig. 3E) than a Himalayan-style channel (Jamieson et al. 2007).

IMPLICATIONS FOR MOUNTAIN-BUILDING PROCESSES

The experimental results, computer models, and geophysical and geological data described above demonstrate that melting has a profound effect on rock strength, that melt-weakening strongly influences the tectonic style of mountain belts, that weak partial-melt zones and magma are present within large modern orogens, and that protracted interaction among melting, deformation, and crustal flow can be documented in both modern and ancient orogenic belts. While mountain building clearly leads to melting, how does melting, once initiated, affect mountain building?

Plate convergence at rates of 1–5 cm/y initially forms "small cold orogens" (Fig. 7), with back-to-back wedges (e.g. Willett et al. 1993) consisting largely of low-grade sedimentary and volcanic rocks. As these orogens grow along the "orogenic main sequence" (Fig. 7), thickened crust heats up by radioactive decay on timescales of ca 20 My. When the melt connectivity threshold is reached in a substantial volume of middle and lower crust, steep topographic gradients cannot be sustained and a plateau forms. The orogen must then grow outward rather than upward; that is, melting limits the maximum crustal thickness and elevation of mountain belts.

Where high convergence velocities lead to rapid crustal thickening, an orogen may get very large (≥70 km thick) before it gets hot enough to melt (path 1, Fig. 7). Once melting begins, however, it will affect a substantial volume of crust. The resulting "large hot orogen" will undergo some form of lateral flow, driven by the topographic gradient between the plateau and the undeformed foreland (Fig. 3B). Alternatively, melting may begin when the orogen is still relatively small (≤50 km thick) if the rate of crustal thickening is slow and/or the heating rate is high (e.g. from high concentrations of radioactive elements or injection of mantle-derived magma; cf Clark et al. 2011 this issue). In this case, melting is likely to limit further crustal thickening (path 3), forming a "small hot orogen" characterised by abundant granite plutons intruding upper crustal rocks and anomalously high-grade lower crust. Most orogenic belts probably fall somewhere in between (path 2) and reach moderate thickness (50–70 km) before the onset of widespread melting.

The style of crustal flow will be strongly controlled by factors like heat production and the accumulated volume of melt-prone crust. Once melting begins, absorption of latent heat should tend to buffer crustal temperature (e.g. Clark et al. 2011), and efficient extraction of melt should accompany deformation (e.g. Brown 2007). However, because only a small amount of melt is needed to keep the crust weak (Rosenberg and Handy 2005; Fig. 1B), these factors are unlikely to reverse the melt-weakening process as long as convergence continues and temperature remains within the partial melting range. After convergence stops, thick orogenic crust should remain hot enough to retain some melt for at least 20 My. Large and intermediate orogens may therefore decay by outward flow at their flanks and thinning of their cores (path 4), until flow is inhibited by cooling and reduction of topographic gradients.

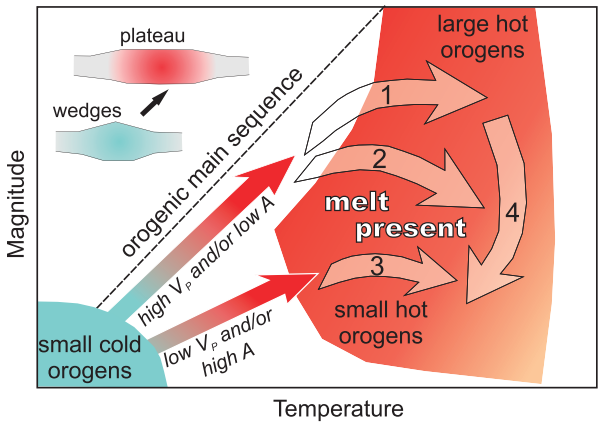

Figure 7 Orogenic temperature–magnitude diagram (after Beaumont et al. 2006) showing how crustal melting (with increasing temperature) may affect the size of orogenic belts as measured by crustal thickness ("magnitude"). V_P = convergence velocity (controls rate of thickening); A = radioactive heat production (controls rate of heating). Red field shows conceptually the region in which dehydration melting is possible, using crustal thickness as a proxy for pressure. Inset shows typical progression along the "orogenic main sequence" (path 1) from back-to-back wedges to large orogens with plateaus.

If crustal melting strongly influences the growth of, and flow within, mountain belts, then the extent of melting can be inferred by examining the Earth's mountain belts, past and present. For example, if orogenic plateaus form in response to melting in the underlying crust, melt should be present beneath the modern Andean and Anatolian plateaus (e.g. Unsworth 2010). In contrast, the rugged topography and relatively small size of the Alps suggest that the degree of crustal melting was insufficient to create a plateau or to drive lateral flow of the middle crust. Finally, to the extent that continental interiors largely consist of the roots of ancient mountain belts, crustal melting has influenced the deep structure of most of the Earth's continental crust.

ACKNOWLEDGMENTS

The authors thank the many colleagues and students who have contributed ideas, data and stimulating discussions over the years (especially C. Beaumont, J. King, M. Handy, P. Štípská), and the funding agencies that have supported our research (including NSERC, NERC and DFG). Constructive comments by principal editor H. McSween, R. Weinberg and an anonymous referee substantially improved the manuscript.

REFERENCES

Arzi AA (1978) Critical phenomena in the rheology of partially melted rocks. Tectonophysics 44: 173-184

Bai D and 12 coauthors (2010) Crustal deformation of the eastern Tibetan plateau revealed by magnetotelluric imaging. Nature Geoscience 3: 358-362

Beaumont C, Jamieson RA, Nguyen MH, Lee B (2001) Himalayan tectonics explained by extrusion of a low-viscosity crustal channel coupled to focused surface denudation. Nature 414: 738-742

Beaumont C, Nguyen MH, Jamieson RA, Ellis S (2006) Crustal flow modes in large hot orogens. In: Law RD, Searle MP, Godin L (eds) Channel Flow, Ductile Extrusion and Exhumation of Lower Mid-crust in Continental Collision Zones. Geological Society of London Special Publication 268, pp 91-145

Brown M (2007) Crustal melting and melt extraction, ascent and emplacement in orogens: mechanisms and consequences. Journal of the Geological Society 164: 709-730

Clark C, Fitzsimons ICW, Healy D, Harley SL (2011) How does the continental crust get really hot? Elements 7: 235-240

Clark MK, Royden LH (2000) Topographic ooze: Building the eastern margin of Tibet by lower crustal flow. Geology 28: 703-706

Costa A, Caricchi L, Bagdassarov N (2009) A model for the rheology of particle-bearing suspensions and partially molten rocks. Geochemistry, Geophysics, Geosystems 10: Q03010, doi:10.1029/2008GC002138

Gerya TV, Perchuk LL, Burg J-P (2008) Transient hot channels: Perpetrating and regurgitating ultrahigh-pressure, high-temperature crust–mantle associations in collision belts. Lithos 103: 236-256

Harris N (2007) Channel flow and the Himalayan–Tibetan orogen: a critical review. Journal of the Geological Society 164: 511-523

Harris N, Massey J (1994) Decompression and anatexis of Himalayan metapelites. Tectonics 13: 1537-1546

Jamieson RA, Beaumont C, Medvedev S, Nguyen MH (2004) Crustal channel flows: 2. Numerical models with implications for metamorphism in the Himalayan-Tibetan orogen. Journal of Geophysical Research 109: B06407, doi:10.1029/2003JB002811

Jamieson RA, Beaumont C, Nguyen MH, Grujic D (2006) Provenance of the Greater Himalayan Sequence and associated rocks: predictions of channel flow models. In: Law RD, Searle MP, Godin L (eds) Channel Flow, Ductile Extrusion and Exhumation of Lower Mid-crust in Continental Collision Zones. Geological Society of London Special Publication 268, pp 165-182

Jamieson RA, Beaumont C, Nguyen MH, Culshaw NG (2007) Synconvergent ductile flow in variable-strength continental crust: Numerical models with application to the western Grenville orogen. Tectonics 26: TC5005, doi:10.1029/2006TC002036

King J, Harris N, Argles T, Parrish R, Zhang HF (2011) Contribution of crustal anatexis to the tectonic evolution of Indian crust beneath southern Tibet. Geological Society of America Bulletin 123: 218-239

Klemperer SL (2006) Crustal flow in Tibet: geophysical evidence for the physical state of Tibetan lithosphere, and inferred patterns of active flow. In: Law RD, Searle MP, Godin L (eds) Channel Flow, Ductile Extrusion and Exhumation of Lower Mid-crust in Continental Collision Zones. Geological Society of London Special Publication 268, pp 39-70

Lexa O, Schulmann K, Janoušek V, Štípská P, Guy A, Racek M (2011) Heat sources and trigger mechanisms of exhumation of HP granulites in Variscan orogenic root. Journal of Metamorphic Geology 29: 79-102

Nábělek J, Hetényi G, Vergne J, Sapkota S, Kafle B, Jiang M, Su H, Chen J, Huang B-S, Hi-CLIMB Team (2009) Underplating in the Himalaya-Tibet collision zone revealed by the Hi-CLIMB experiment. Science 325: 1371-1374

Nelson KD and 27 coauthors (1996) Partially molten middle crust beneath southern Tibet: Synthesis of project INDEPTH results. Science 274: 1684-1688

Paterson MS (2001) A granular flow theory for the deformation of partially melted rock. Tectonophysics 335: 51-61

Rey PF, Teyssier C, Whitney DL (2009) Extension rates, crustal melting, and core complex dynamics. Geology 37: 391-394

Rosenberg CL, Handy MR (2005) Experimental deformation of partially melted granite revisited: implications for the continental crust. Journal of Metamorphic Geology 23: 19-28

Rosenberg CL, Medvedev S, Handy M (2007) On the effects of melting on continental deformation and faulting. In: Handy M, Hirth G, Hovius N (eds) Tectonic Faults: Agents of Change on a Dynamic Earth. Dahlem Workshop Report 95, MIT Press, pp 357-402

Royden LH, Burchfiel BC, van der Hilst RD (2008) The geological evolution of the Tibetan Plateau. Science 321: 1054-1058

Schulmann K, Lexa O, Štípská P, Racek M, Tajčmanová L, Konopásek J, Edel J-B, Peschler A, Lehmann J (2008a) Vertical extrusion and horizontal channel flow of orogenic lower crust: key exhumation mechanisms in large hot orogens? Journal of Metamorphic Geology 26: 273-297

Schulmann K, Martelat J-E, Ulrich S, Lexa O, Štípská P, Beckers JK (2008b) Evolution of microstructure and melt topology in partially molten granitic mylonite: Implications for rheology of felsic middle crust. Journal of Geophysical Research 113: B10406, doi:10.1029/2007JB005508

Schulmann K, Konopásek J, Janoušek V, Lexa O, Lardeaux J-M, Edel J-B, Štípská P, Ulrich S (2009) An Andean type Palaeozoic convergence in the Bohemian Massif. Comptes Rendus de l'Académie des Sciences Geosciences 341: 266-286

Slagstad T, Jamieson RA, Culshaw NG (2005) Formation, crystallization, and migration of melt in the mid-orogenic crust: Muskoka domain migmatites, Grenville Province, Ontario. Journal of Petrology 46: 893-919

Unsworth M (2010) Magnetotelluric studies of active continent-continent collisions. Surveys in Geophysics 31: 137-161

Unsworth MJ, Jones AG, Wei W, Marquis G, Gokarn SG, Spratt JE (2005) Crustal rheology of the Himalaya and Southern Tibet inferred from magnetotelluric data. Nature 438: 78-81

Willett SD, Beaumont C, Fullsack P (1993) Mechanical model for the tectonics of doubly vergent compressional orogens. Geology 21: 371-374

Zhang H, Harris N, Parrish R, Kelley S, Zhang L, Rogers N, Argles T, King J (2004) Causes and consequences of protracted melting of the mid-crust exposed in the North Himalayan antiform. Earth and Planetary Science Letters 228: 195-212